Oceanologia (2017) 59, 271—282

Available online at www.sciencedirect.com

ScienceDirect

journal homepage: www.journals.elsevier.com/oceanologia/

ORIGINAL RESEARCH ARTICLE

# Chromophoric dissolved organic matter (CDOM) variability over the continental shelf of the northern Bay of Bengal

Sourav Das [a,*], Isha Das [a], Sandip Giri [a], Abhra Chanda [a], Sourav Maity [b], Aneesh A. Lotliker [b], T. Srinivasa Kumar [b], Anirban Akhand [c], Sugata Hazra [a]

[a] School of Oceanographic Studies, Jadavpur University, Kolkata, India
[b] Indian National Centre for Ocean Information Services, Kukatpally, Hyderabad, India
[c] Coastal and Estuarine Environment Research Group, Port and Airport Research Institute, Nagase, Yokosuka, Japan

Received 19 September 2016; accepted 6 March 2017
Available online 22 March 2017

**KEYWORDS**
$a_{CDOM}(440)$;
Spatio-temporal variability;
Sea surface salinity;
Northern Bay of Bengal

**Summary** The present paper dealt with the annual dynamics of the absorption coefficient of chromophoric dissolved organic matter at 440 nm {$a_{CDOM}(440)$} during February 2015 to January 2016 in the continental shelf of northern Bay of Bengal (nBoB) for the first time. Sea surface salinity (SSS), chlorophyll-*a* (Chl-*a*), total suspended matter (TSM) were also analyzed. It was hypothesized that CDOM should exhibit significant spatial and temporal variability in this region. $a_{CDOM}(440)$ and spectral slope ranged between 0.1002 $m^{-1}$—0.6631 $m^{-1}$ and 0.0071 $nm^{-1}$—0.0229 $nm^{-1}$ respectively during the entire study period. Higher values of $a_{CDOM}(440)$ were observed in the near shore stations and gradually decreased towards the offshore. Significant seasonal variability of $a_{CDOM}(440)$ was observed between the monsoon and non-monsoon seasons ($p < 0.05$). Thus the framed hypothesis was successfully accepted by means of the present study. The CDOM was mainly found to be of allochthonous character in this region. $a_{CDOM}(440)$ portrayed a significant negative linear relationship with SSS ($R^2 = 0.80$; $p < 0.05$) implying conservative mixing of marine and terrestrial end members. However, examining the spatial variability of the relationship, it was observed that this relationship was significant only in the nearshore stations.

* Corresponding author at: School of Oceanographic Studies, Jadavpur University, Jadavpur, 188 Raja S.C. Mullick Road, Kolkata 700032, West Bengal, India. Tel.: +91 33 2414 6242; fax: +91 33 2414 6242.
*E-mail address:* sourav.biooptics@gmail.com (S. Das).
Peer review under the responsibility of Institute of Oceanology of the Polish Academy of Sciences.

Production and hosting by Elsevier

http://dx.doi.org/10.1016/j.oceano.2017.03.002

While examining the seasonal variability of this relationship, it was found to be most significant during the monsoon ($R^2$ = 0.81; $p < 0.05$). Thus it was inferred that whenever the SSS gradient was higher, the relationship between $a_{CDOM}(440)$ and SSS was found to be most significant.


## 1. Introduction

The ability of coastal water to transmit sunlight to planktonic, macrophytic and other submerged vegetation for photosynthesis is one of the prime indicators of the health of coastal ecosystems. Chromophoric dissolved organic matter (CDOM) is one of the major light-absorbing constituents of the coastal waters. CDOM is found in all types of natural waters and it is capable of changing the colour of the water (Blough and Del Vecchio, 2002). It consists of a varied mixture of aliphatic and aromatic polymers that are mostly derived from the degradation of terrestrial and aquatic plant matter (Kirk, 1994). Its absorption is strongest in the ultraviolet (UV) region (Stedmon et al., 2000). This strong absorption of UV radiation by CDOM prevents the phytoplankton and other biota from being damaged in the coastal ecosystems (Blough and Zepp, 1990; Blough and Green, 1995). In higher concentration, CDOM absorption can alter the primary productivity of a coastal ecosystem by reducing the availability of photosynthetically active radiation to the phytoplankton community (Bidigare et al., 1993). Several studies were carried out on the colour signal of CDOM from the perspective of remote sensing applications, where the effect of CDOM was considered while measuring the phytoplankton and suspended sediment by means of remotely sensed data (Karabashev, 1992; Tassan, 1988). The optical characteristics of coastal and estuarine waters have a complex nature and they exhibit significant temporal and spatial variability of CDOM concentration (Keith et al., 2002). CDOM concentrations increase in coastal waters due to the anthropogenic input of industrial or domestic effluents by river discharges (Bricaud et al., 1981) along with in situ production from phytoplankton debris (Carder et al., 1989). The optical properties of CDOM also change due to the mixing of seawater with freshwater and phenomenon like photo-degradation in the coastal regions (Bricaud et al., 1981; Carder et al., 1989; Del Castillo et al., 2000; Morel, 1988; Vodacek et al., 1997).

From the perspective of characterizing the CDOM variability, very few studies are reported from the northern Bay of Bengal (nBoB) (Das et al., 2016a, 2016b). The CDOM dynamics is expected to be highly variable due to the biogeochemical complexity of this study region (Biswas et al., 2010; Mukhopadhyay et al., 2006). However, the CDOM variability data in this study region is available only for post-monsoon season (Das et al., 2016a, 2016b). In the short term study, Das et al. (2016a) walso described that among the selected physico-chemical parameters, salinity exhibited significant correlation with the absorption coefficient of CDOM at 440 nm [$a_{CDOM}(440)$] during the post-monsoon season in this study region.

Owing to the existing scarcity of spatial and temporal (especially annual) data in the present study region, we have framed this study and hypothesized that magnitudes of CDOM vary both spatially and temporally in the near shore to the offshore transition zone of nBoB. The absorption coefficient of CDOM was measured at 440 nm [i.e., $a_{CDOM}(440)$] since it is implemented directly in various remote sensing applications. The first objective of the present study (in accordance with the proposed hypothesis) was to examine the spatial and temporal (monthly or seasonal) variability of CDOM throughout one annual cycle (February 2015—January 2016). The second objective of the study was to determine whether the CDOM in this region is autochthonous or allochthonous in nature. The third objective was to examine that whether the pre-existing relationship between CDOM and salinity observed by Das et al. (2016a) during their short term work holds true for the entire annual cycle or not in the present study region.

## 2. Study area

The present study was conducted in the near shore to offshore transition zone of nBoB (Fig. 1). This study region is located in the shallow continental shelf (<20 m bottom depth) off the coastline of the state of West Bengal, India. This area receives a substantial amount of freshwater discharge as well as total suspended matter (TSM) from the perennial River Hugli flowing by the megacities of Kolkata and Howrah (Das et al., 2015; Mukhopadhyay et al., 2006). Therefore, a substantial amount of terrestrial organic matter mixes in the present study region all through the year. This discharge peaks during monsoon (Unger et al., 2003; Varkey et al., 1996). The present study area receives the freshwater flow mainly from the Farakka Barrage situated 286 km upstream from the Hugli River mouth (Biswas et al., 2010). Moreover, it is also bounded by the Sundarban mangrove ecosystem in the north. There are several other tidally influenced distributaries within the Sundarban mangroves like Saptamukhi, Thakuran, Matla, Gosaba and Bidya (from west to east) which act as a source of organic matter into the study region (Das et al., 2015). This region is characterized by an intense semidiurnal tide of meso-macrotidal nature (2.5—7 m) (De et al., 2011). The study site is also affected by episodic events, such as heavy precipitation associated with land drainage, cyclones and seasonal coastal upwelling, that bring significant quantities of nutrients to the photic layer (Maneesha et al., 2011) along with detritus loads. Previous studies also revealed that the present study region experiences a significant prevalence of organic matter (Biswas et al., 2010; Mukhopadhyay et al., 2006). The climate in this part of the world is demarcated as pre-monsoon (February—May), monsoon (June—September) and post-monsoon (October—January). About 70—80% of the rainfall occurs between June and September (Mukhopadhyay et al., 2006). The south west monsoon driven rainfall enhances

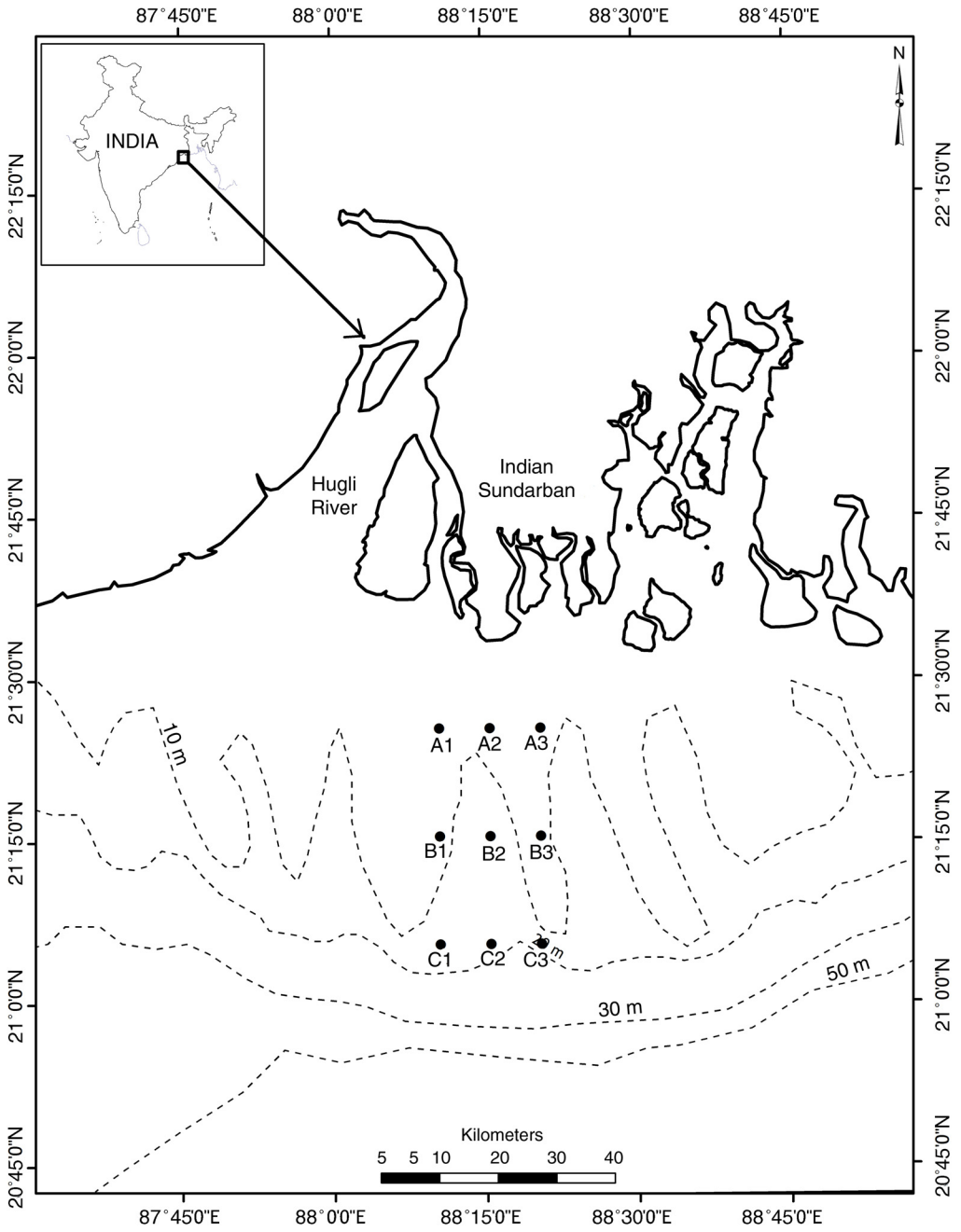


**Figure 1** The study area map showing the sampling locations in the shallow continental shelf waters of the nBoB.

the freshwater discharge rate in the nBoB, whereas, during the pre-monsoon and the post-monsoon seasons the freshwater flow remains comparatively lean (Rudra, 2014).

## 3. Material and method

### 3.1. Sampling plan

In order to examine the spatial variability in the nBoB during the study period, the sampling tracks were divided into three transects: near shore (A1, A2 and A3 collectively referred to as 'A transect'), middle (B1, B2 and B3 collectively referred to as 'B transect') and offshore (C1, C2 and C3 collectively referred to as 'C transect'). In total the present survey was conducted at nine stations (Table 1) throughout one annual cycle (February 2015—January 2016). All the cruises were begun from Frasargunje Fishing Harbour (Lat. 21°34′45″N; Long. 88°15′05″E). During the present study period a total of twelve sampling surveys were carried out. One survey was conducted in the first week of each month and one sample (mean of triplicate samples were considered for each parameter) was taken from each sampling point during all those surveys. Hence throughout the annual cycle, 108 samples were collected in total. The entire sampling was accomplished in the daytime only. Seawater samples were collected

**Table 1** Geographical location of sampling stations.

| Sampling station | Latitude (N) | Longitude (E) |
|---|---|---|
| A1 | 21°25′30″ | 88°10′30″ |
| A2 | 21°25′30″ | 88°15′30″ |
| A3 | 21°25′30″ | 88°20′30″ |
| B1 | 21°15′30″ | 88°10′30″ |
| B2 | 21°15′30″ | 88°15′30″ |
| B3 | 21°15′30″ | 88°20′30″ |
| C1 | 21°05′30″ | 88°10′30″ |
| C2 | 21°05′30″ | 88°15′30″ |
| C3 | 21°05′30″ | 88°20′30″ |

using a Niskin Sampler (General Oceanics, Inc.) from the water surface (0.25 m below the air–water interface). Sea surface temperature (SST) and sea surface salinity (SSS) were analyzed immediately onboard. Samples were transferred into pre-rinsed amber coloured plastic containers from the Niskin sampler for TSM and chlorophyll-*a* (chl-*a*) analysis. CDOM was sampled according to Sasaki et al. (2005).

### 3.2. Analytical protocol

SSS and SST were measured using a Multikit (WTW Multi 340 i Set; Merck, Germany) fitted with the probe WTW Tetracon 325. In order to measure chl-*a* content, 2 L of each sample was passed through GF/F (Whatman, 47 mm diameter) glass-fibre filter onboard and the filters were stored in liquid nitrogen cylinder while bringing back to laboratory until further analysis. The chl-*a* samples were extracted in 10 ml 90% acetone and measured using a UV-vis spectrophotometer (Shimadzu UV-visible 1600 double-beam) following a standard protocol (Parson et al., 1984; Suzuki and Ishimaru, 1990). In order to measure TSM, a well-mixed sample was filtered through a weighed standard glass-fibre filter (pore size: 0.45 μM) and the residue retained on the filter was dried to a constant weight at 103–105°C. Filter papers were weighed by using Electronic Balance (Denver Instrument, Germany) having a precision of 0.0001 g. TSM was calculated by using the equation: TSM [g $m^{-3}$] = $(A - B) \times 1000/C$ (Strickland and Parsons, 1972), where, $A$ = (weight of filter + dried residue) [g], $B$ = weight of filter [g], $C$ = volume of water filtered [$m^3$].

For CDOM absorption, the seawater samples were stored in amber coloured glass bottles for four hours to equilibrate to room temperature. The samples were filtered through the 47 mm Whatman GF/F filter to remove the coarse particles. The filtered seawater samples were again filtered through 47 mm Nuclepore membrane filter (pore size: 0.2 μm) to remove the fine particles. The absorption of CDOM was scanned in the range from 300 to 750 nm using 10 cm path-length cuvette with UV-VIS spectrophotometer (Shimadzu UV-Visible 1600 double-beam). Milli-Q water was used as a reference. The measured absorbance data were normalized to zero at 600 nm due to temperature-dependent artefacts (Pegau and Zaneveld, 1993) observed between 650 nm and 750 nm. A blank (Milli-Q water versus Milli-Q water) was subtracted from each wavelength of the spectrum. The CDOM absorbance was then multiplied by 2.303 to convert from $\log_{10}$ to $\log_e$ and by 10 to convert to a 1 m pathlength (Sasaki et al., 2005). The CDOM absorption coefficients were obtained by the following equation:

$$a(\lambda) = 2.303 \times \frac{D(\lambda)}{L},$$

where $\lambda$ is the wavelength and $L$ is the cuvette length in metres. $a(\lambda)$ is the absorption coefficient at wavelength $\lambda$, and $D(\lambda)$ is the absorbance at wavelength $\lambda$.

The value of spectral slope of CDOM absorption (S) has most often been determined using an exponential regression (Bricaud et al., 1981; Jerlov, 1968) since non-linear regression fitting provides a better estimate of S, by weighting

**Table 2** Mean ± standard deviation from mean along with minimum and maximum value (within parentheses) of the annual data set for the parameters SSS, TSM, Chl-*a*, $a_{CDOM}(440)$ along with the linear regression equation between SSS and $a_{CDOM}(440)$ obtained from the respective sampling stations.

| Site | SSS | TSM [g $m^{-3}$] | Chl-*a* [mg $m^{-3}$] | $a_{CDOM}(440)$ [$m^{-1}$] | Linear regression equation | $R^2$ |
|---|---|---|---|---|---|---|
| A1 | 23.1 ± 5.7 (14.5–29.6) | 46.7 ± 15.7 (27.3–80.8) | 0.92 ± 0.39 (0.35–1.66) | 0.3069 ± 0.1991 (0.1111–0.6631) | SSS = −27.53 × $a_{CDOM}(440)$ + 31.50 | 0.92 |
| A2 | 24.6 ± 5.6 (15.1–30.6) | 46.5 ± 16.3 (26.8–82.6) | 0.82 ± 0.43 (0.29–1.88) | 0.2341 ± 0.1797 (0.1022–0.6195) | SSS = −27.64 × $a_{CDOM}(440)$ + 31.02 | 0.80 |
| A3 | 26.6 ± 3.7 (20.3–30.9) | 42.0 ± 15.0 (25.1–74.2) | 0.78 ± 0.24 (0.44–1.33) | 0.1519 ± 0.0698 (0.1002–0.3195) | SSS = −38.66 × $a_{CDOM}(440)$ + 32.51 | 0.52 |
| B1 | 23.8 ± 5.8 (14.9–30.2) | 42.0 ± 10.3 (26.5–57.4) | 0.88 ± 0.26 (0.55–1.50) | 0.2796 ± 0.1809 (0.1022–0.6332) | SSS = −30.35 × $a_{CDOM}(440)$ + 32.31 | 0.91 |
| B2 | 26.0 ± 4.0 (19.2–30.5) | 40.9 ± 12.1 (23.7–59.3) | 0.86 ± 0.33 (0.55–1.63) | 0.1620 ± 0.0877 (0.1015–0.3562) | SSS = −37.33 × $a_{CDOM}(440)$ + 32.00 | 0.66 |
| B3 | 25.3 ± 5.5 (15.5–30.8) | 39.9 ± 15.9 (21.7–64.9) | 0.80 ± 0.23 (0.55–1.38) | 0.1631 ± 0.0877 (0.1011–0.3551) | SSS = −58.64 × $a_{CDOM}(440)$ + 34.87 | 0.89 |
| C1 | 28.5 ± 3.6 (23.5–32.6) | 10.0 ± 2.0 (8.3–15.7) | 1.20 ± 0.91 (0.51–3.22) | 0.1558 ± 0.0557 (0.1011–0.2522) | SSS = −29.07 × $a_{CDOM}(440)$ + 33.05 | 0.20 |
| C2 | 28.6 ± 3.6 (23.3–32.9) | 10.1 ± 2.1 (8.2–15.6) | 1.44 ± 1.11 (0.61–3.69) | 0.1561 ± 0.0564 (0.1012–0.2562) | SSS = −27.44 × $a_{CDOM}(440)$ + 32.84 | 0.18 |
| C3 | 28.7 ± 3.3 (23.8–33.1) | 11.0 ± 2.0 (8.9–16.5) | 1.33 ± 0.94 (0.69–3.55) | 0.1556 ± 0.0553 (0.1011–0.2522) | SSS = −26.23 × $a_{CDOM}(440)$ + 32.76 | 0.19 |

regions of higher CDOM absorption (Stedmon et al., 2000). Here, S was determined after applying a non-linear exponential regression (Para et al., 2010) to original $a_{CDOM}(\lambda)$ data measured within the range 400–600 nm. All the determination coefficients ($R^2$) calculated from these exponential fits were always >0.98. S provides information concerning CDOM origin (terrestrial versus marine), with generally lower slopes in fresh and coastal waters than in the open ocean due to the presence of marine humics and new biological CDOM (Blough and Del Vecchio, 2002; Ferrari, 2000).

### 3.3. Statistical analysis

The Pearson correlation coefficient ($r$) was computed and regression models were tested between $a_{CDOM}(440)$ and SSS, TSM, chl-*a* and slope. A one-way analysis of variance (ANOVA) was used to test the differences in mean of the respective parameters in different seasons and different transects. All statistical analysis was conducted using SPSS version 13.0.

### 3.4. Ancillary data used

The measurement of Hugli River discharge (especially from Farakka Barrage) is restricted by the Govt. of India. However, in order to correlate the monthly CDOM concentration with monthly Hugli River discharge, we have used the data set of Rudra (2014) which was derived from a rainfall-runoff model. The monthly mean rainfall (in mm) was obtained from the Tropical Rainfall Measuring Mission (TRMM) 3B43 (V7) product downloaded from http://giovanni.sci.gsfc.nasa.gov. The present data constitutes the monthly combined microwave-IR-gauge estimates of precipitation computed on quasi-global grids. The total rainfall surrounding ≈ 50 km buffer area of the Hugli Estuary starting from the Farakka Barrage has been taken into account during the period February 2015 to January 2016.

## 4. Results

### 4.1. Overall hydrography of the study region

SST during the sampling period varied over a range of ~21.2°C to ~28.8°C. The seasonal mean SST were 25.3 ± 2.4°C, 27.1 ± 1.0°C and 22.1 ± 2.3°C during pre-monsoon, monsoon and post-monsoon season respectively. No spatial trend of SST was observed during the study period. The SSS values ranged from 14.5 to 33.1 during the annual course of sampling (see Table 2 for details). A significant seasonal variability in SSS was observed. The SSS values were highest in the pre-monsoon season (30.0 ± 1.2) followed by the post-monsoon season (27.1 ± 4.1). The lowest was observed during the monsoon months (21.3 ± 3.7). SSS was found much higher in the offshore stations (C1, C2 and C3) than the inshore stations (A1, A2 and A3) throughout the annual period of sampling (Fig. 2a). TSM concentrations were higher during the monsoon (43.3 ± 23.7 g $m^{-3}$) followed by the post-monsoon (28.6 ± 15.3 g $m^{-3}$) and pre-monsoon season (24.6 ± 11.9 g $m^{-3}$). Seasonal mean chl-*a* values as low as 0.88 ± 0.20 mg $m^{-3}$ was observed during monsoon. The highest seasonal mean chl-*a* concentration was 1.14 ± 0.80 mg $m^{-3}$ in post-monsoon (Fig. 2b). Chl-*a* did not show any significant spatial trend in this study region.

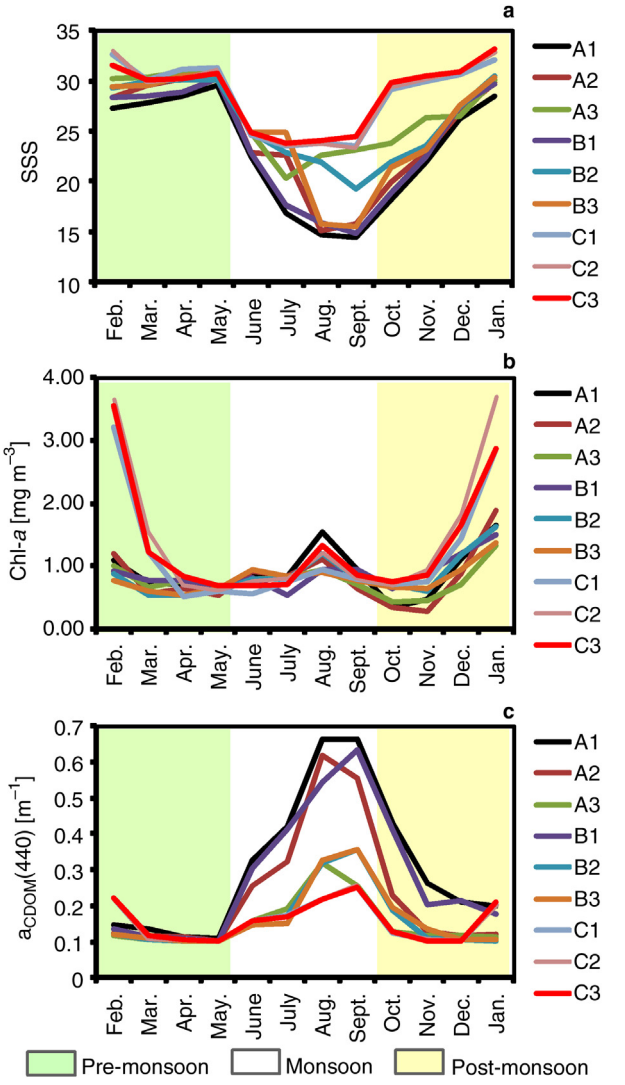


**Figure 2** Spatio-temporal variability of (a) SSS, (b) Chl-*a* and (c) $a_{CDOM}(440)$ of different sampling stations during study time.

### 4.2. Spatio-temporal distribution of light absorption characteristics of CDOM

The $a_{CDOM}(440)$ varied between 0.1002 $m^{-1}$ and 0.6631 $m^{-1}$ during the entire study period. Seasonal mean $a_{CDOM}(440)$ (considering all the data) exhibited a marked difference in magnitudes in the three seasons (one-way ANOVA: $F = 11.77$, $p < 0.05$). It was as low as 0.1200 ± 0.0327 $m^{-1}$ during the pre-monsoon, which increased to 0.3064 ± 0.1595 $m^{-1}$ in the monsoon season and in the post-monsoon it was 0.1621 ± 0.0790 $m^{-1}$. While analysing the spatial distribution higher values of $a_{CDOM}(440)$ were observed near the confluence (A1, A2 and A3) and a gradual decrease towards the offshore (C1, C2 and C3) was observed (Fig. 2c) except post-monsoon season (one-way ANOVA: $F = 2.99$, $p < 0.05$). Results also showed that magnitude of $a_{CDOM}(440)$ was almost half in A3 (0.1519 ± 0.0698 $m^{-1}$) compared to A1

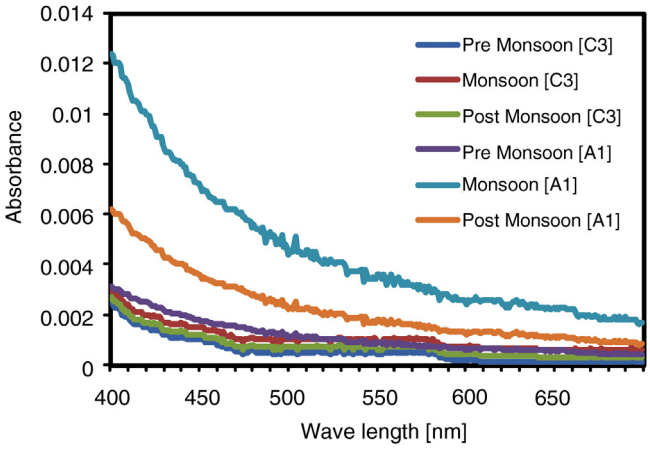


**Figure 3** Absorption spectra of CDOM at two stations, representing the near shore water (A1) and offshore water (C3) during pre-monsoon (3rd April, 2015), monsoon (5th August, 2015) and post-monsoon (7th January, 2016) season respectively.

($0.3069 \pm 0.1991\ m^{-1}$), i.e. $a_{CDOM}(440)$ showed decreasing trend from west towards the east (Table 2). The absorption spectra of CDOM obtained at the stations A1 and C3 in three distinct seasons are portrayed in Fig. 3.

The spectral slope values (S) ranged between 0.0071 $nm^{-1}$ and 0.0229 $nm^{-1}$ during the entire study. Mean slope was lower ($0.0123 \pm 0.0026\ nm^{-1}$) during monsoon and higher ($0.0185 \pm 0.0043\ nm^{-1}$) in the pre-monsoon season. However, seasonal mean slope did not show significant difference during the study period (one-way ANOVA: $F = 0.75$, $p = 0.48$). The spatial distribution of slope exhibited that mean slope was significantly higher in the offshore stations compared to the inshore ones (one-way ANOVA: $F = 1.79$, $p < 0.05$). Slope and $a_{CDOM}(440)$ exhibited a statistically significant negative exponential relationship among each other in all the three seasons. The coefficient of determination was found highest during the pre-monsoon season ($R^2 = 0.93$, $p < 0.05$) and monsoon season ($R^2 = 0.93$, $p < 0.05$) followed by the post-monsoon season ($R^2 = 0.87$, $p < 0.05$) (Fig. 4a–c).

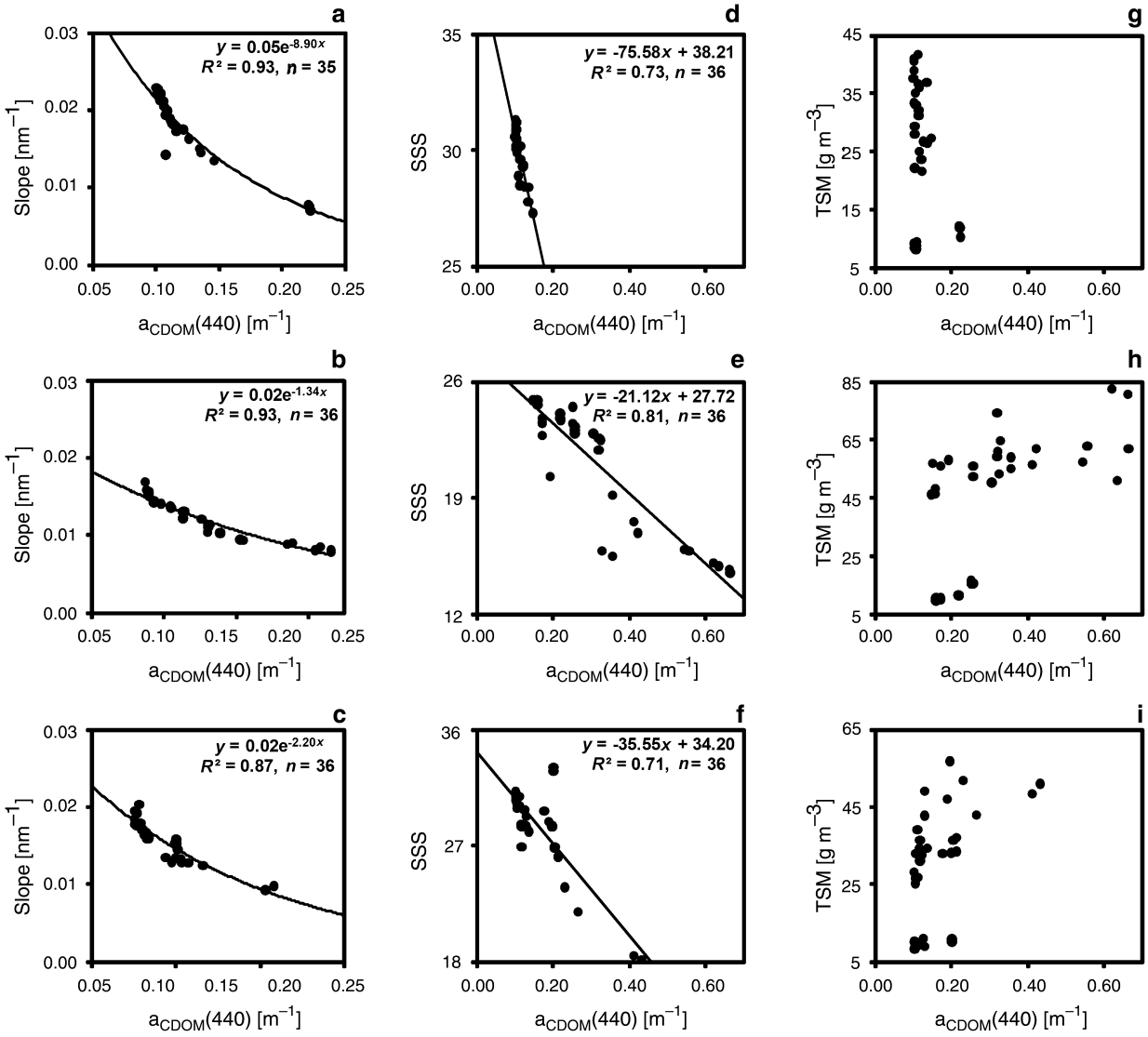


**Figure 4** Correlation between $a_{CDOM}(440)$ with slope, SSS and TSM (top, middle and bottom row indicating pre-monsoon, monsoon and post-monsoon season respectively).

### 4.3. Relationship between CDOM and other relevant hydrographical parameters

The calculated Pearson correlation coefficient squared ($R^2$) between $a_{CDOM}(440)$ and SSS, TSM and chl-*a* (considering the entire dataset obtained from this study) depicted significant linear relation between $a_{CDOM}(440)$ and SSS. $a_{CDOM}(440)$ did not show any such significant relationship with chl-*a* and TSM. Considering the annual data set, $a_{CDOM}(440)$ was related with SSS according to the equation $SSS = -\{32.45 \times a_{CDOM}(440)\} + 32.75$ ($R^2 = 0.80$, $p < 0.05$). Upon analysing the seasonal data, the strongest statistically significant negative correlation was observed between $a_{CDOM}(440)$ and SSS during monsoon ($R^2 = 0.88$, $N = 36$, $p < 0.001$) followed by post-monsoon ($R^2 = 0.81$, $N = 36$, $p < 0.001$) and pre-monsoon ($R^2 = 0.73$, $N = 36$, $p < 0.001$) (Fig. 4d–f). However, $a_{CDOM}(440)$ did not exhibit any correlation with chl-*a* and TSM (Fig. 4g–i) during any of the seasons.

While analysing the spatial variability of the relationships between CDOM and the above-mentioned parameters, it was observed that the relationship between $a_{CDOM}(440)$ and SSS was found significant in the near shore stations (A and B transect) and the relationship was not significant in the offshore stations (C transect) (see Table 2). Though all the near shore stations showed a significant correlation between $a_{CDOM}(440)$ and SSS, the $R^2$ value between SSS and $a_{CDOM}(440)$ showed a decreasing trend from west to east (A1–A3) direction. Correlation analysis did not show any significant relationship between $a_{CDOM}(440)$ and chl-*a* in the offshore (C3) as well as an inshore station (A1) (Fig. 5). Significant positive correlation was observed between $a_{CDOM}(440)$ and TSM in both the stations (Fig. 6).

### 4.4. Variation in CDOM absorption with freshwater discharge and rainfall

Inspection of the monthly Hugli River discharge vs. $a_{CDOM}(440)$ time series indicated that a significant positive relationship might exist between the two parameters at inshore stations ($R^2 = 0.81$, $p < 0.05$) (Fig. 7a and b), whereas, in the offshore station the relationship was not significant (Fig. 7c). Correlation between rainfall and $a_{CDOM}(440)$ time series data also showed the same trend as observed in the case of discharge vs. $a_{CDOM}(440)$. Significant positive correlation between rainfall and $a_{CDOM}(440)$ was observed at the inshore station ($R^2 = 0.63$; $p < 0.05$) (Fig. 7d and e), however, at the offshore station it was not significant (Fig. 7f).

## 5. Discussion

The study area encompasses a typical freshwater-seawater mixing regions of the world. The immense freshwater input from the Ganga-Brahmaputra-Meghna (GBM) River System accompanied by sediment load (Mukhopadhyay et al., 2006) gets diluted in this area by means of mixing with seawater of the nBoB. The general hydrography in such near

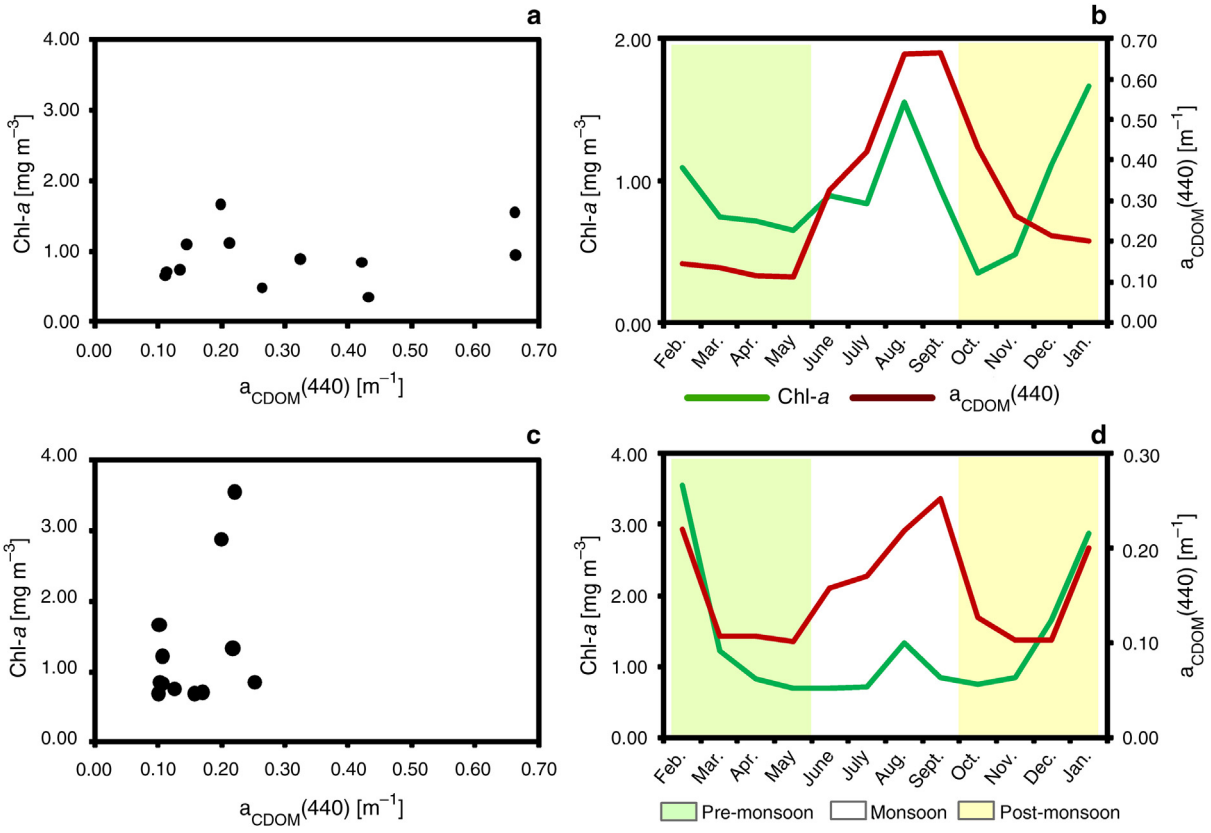


**Figure 5** Correlation between $a_{CDOM}(440)$ and Chl-*a* at sampling station A1 (a, b) and C3 (c, d).

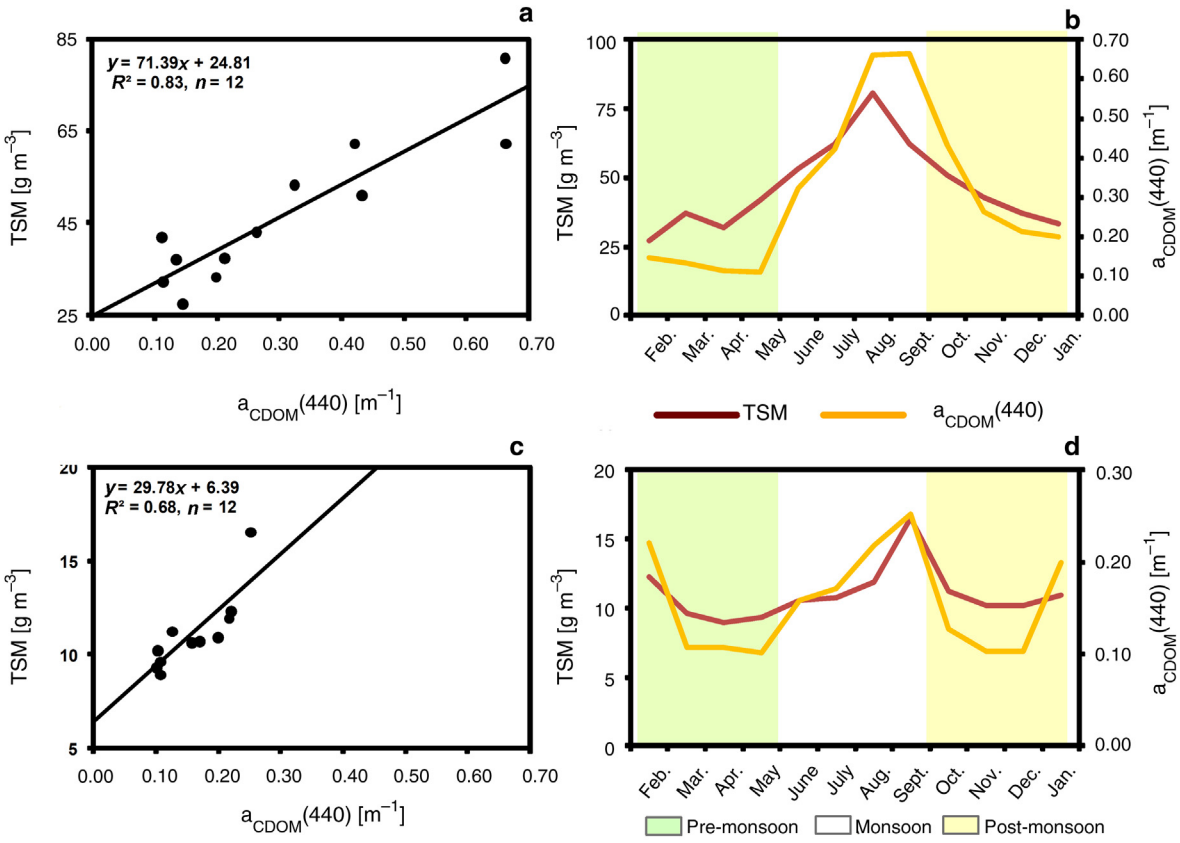


**Figure 6** Correlation between $a_{CDOM}(440)$ and TSM at sampling station A1 (a, b) and C3 (c, d).

shore to offshore transition zones is principally characterized by this mixing process along with the stratification in water column (Luyten et al., 1996) and eventually it leads to the formation of an extended continental shelf having a very shallow depth in nBoB. It was observed from the results depicted in Section 4.1 that this region experiences significant seasonal variation in hydrographical parameters and it was thus expected to vary the seasonal $a_{CDOM}(440)$ as well (Lin et al., 2012).

Most significant temporal variations were observed in TSM and SSS values especially between the monsoon and non-monsoon months. Though GBM acts as a perennial source of freshwater supply in this region its freshwater input increases during the peak of the monsoon season. This increased freshwater input resulted in the decrease in SSS and increase in TSM during the monsoon months compared to the non-monsoon months. Chl-*a* magnitudes did not exhibit any significant temporal variability throughout the year except the offshore stations (C transect), where slightly higher values were observed in the post-monsoon season. This might be due to the fact that substantially high sediment load throughout the year might inhibit the photosynthetically active radiation to penetrate the surface layers resulting in limited growth of phytoplankton, especially in the near shore stations. This is further justified as during the post-monsoon season, the offshore stations experienced comparatively lesser TSM influence and hence the higher values of chl-*a* were observed.

$a_{CDOM}(440)$ showed a significant temporal variation in all the stations in parity with the dynamics of SSS and TSM, i.e. significantly higher values were observed in the monsoon season and lower values were found in the other two non-monsoon seasons. Das et al. (2016a) while working at the station A2 observed that $a_{CDOM}(440)$ varied between 0.0862 $m^{-1}$ and 0.2411 $m^{-1}$ during October 2014 to March 2015, while the slope values ranged between 0.0071 and 0.0167 $nm^{-1}$. Whereas, in the present study, during the same duration of months $a_{CDOM}(440)$ varied between 0.1159 $m^{-1}$ and 0.2294 $m^{-1}$ and slope ranged between 0.0094 $nm^{-1}$ and 0.0147 $nm^{-1}$. In the Vishakhapatnam coast situated on the east coast of Bay of Bengal, Pandi et al. (2014) observed $a_{CDOM}(440)$ magnitudes ranging from 0.120 $m^{-1}$ to 0.252 $m^{-1}$, whereas in the present study $a_{CDOM}(440)$ ranged between 0.1002 $m^{-1}$ and 0.6631 $m^{-1}$. Hence it can be seen that the highest $a_{CDOM}(440)$ magnitudes observed in the present study was much higher than the highest magnitudes observed by Pandi et al. (2014). This might be attributed to the vicinity of the present study area to Hugli Estuary, whereas, the study area of Pandi et al. (2014) is far away from the Hugli mouth and it does not experience any significant perennial river flow. Fig. 2 also portrayed that near shore stations showed comparatively higher magnitudes of $a_{CDOM}(440)$ compared to the offshore stations especially during the monsoon season. This might be attributed to the obvious fact that riverine dominance was found much higher in the near shore stations and it steadily dissipated towards the offshore stations. During the monsoon season, mean slope was observed lower than the global average (0.014 $nm^{-1}$) (Del Castillo and Coble, 2000). After analyzing the spatial distribution, it was found

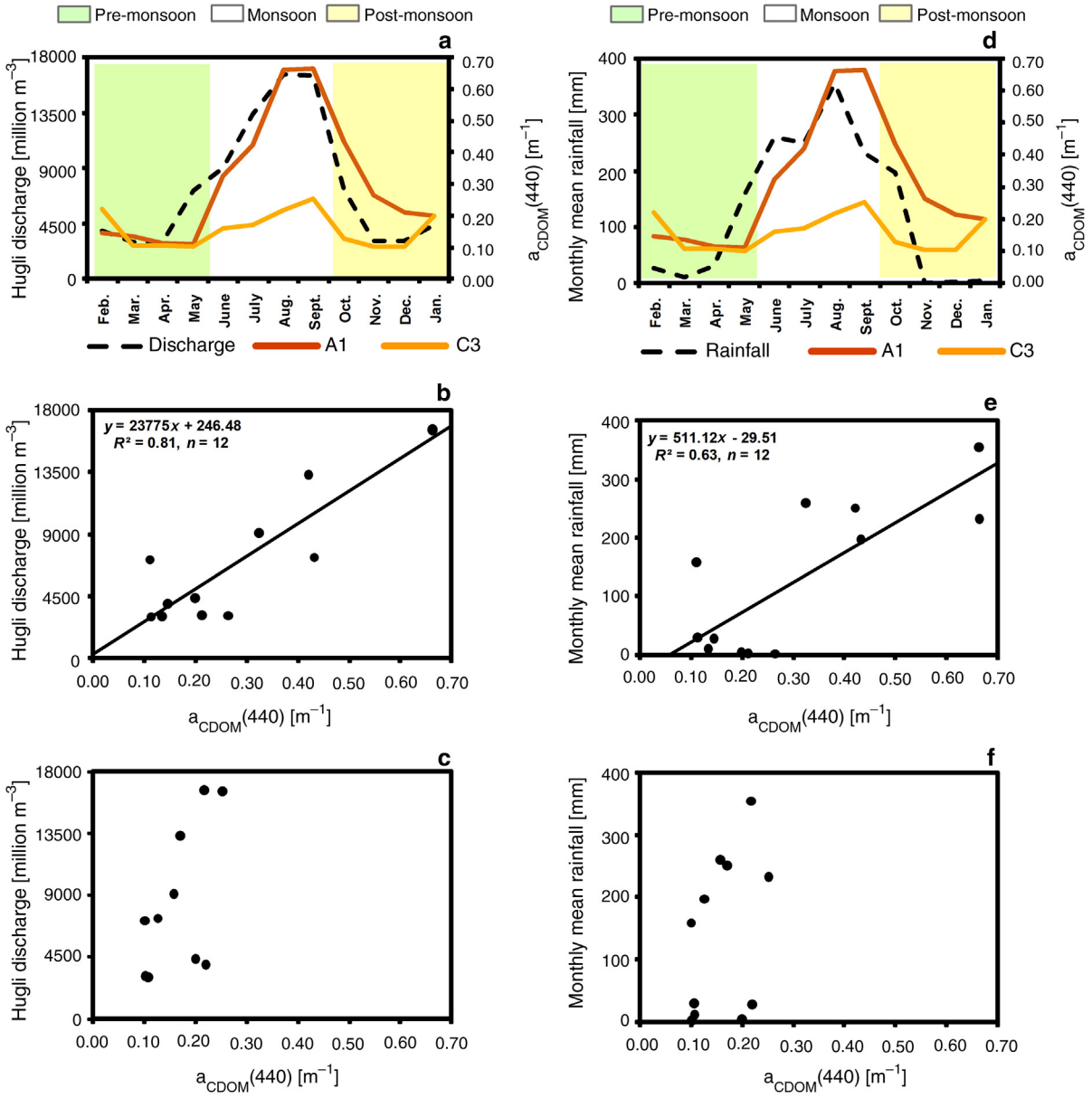


**Figure 7** Line graph between $a_{CDOM}(440)$ at A1 and C3 with (a) Hugli discharge and (d) rainfall. Correlation between $a_{CDOM}(440)$ with Hugli discharge at sampling station A1 (b) and C3 (c) and rainfall at sampling station A1 (e) and C3 (f).

that the near shore stations exhibited lower slope value than the offshore stations all through the study. The lowering of slope values in the near shore stations can be again directly attributed to the strong riverine influence in this region compared to offshore stations. Pandi et al. (2014) while working in north-western BoB observed that CDOM molecular weight increased with dilution led by Hugli's perennial flow (according to Helms et al., 2008; Loiselle et al., 2009), hence it can be similarly inferred that near shore stations of this site comprises of higher molecular weight CDOM compared to offshore stations or the in situ produced DOM (Chen et al., 2011). All these observations strongly advocate the significant spatial and temporal variability of $a_{CDOM}(440)$ in the present study area. Thus the first objective was fulfilled by analyzing these observations, as well as the proposed hypothesis of the present study, was successfully accepted. The present findings along with the observations of Das et al. (2016a, 2016b) and Pandi et al. (2014) also indicated significant evidence of allochthonous character of CDOM in nBOB. Thus the second objective of the present study was also fulfilled.

Das et al. (2016a) in their short term work in nBoB observed that SSS exhibited a significant negative relationship with $a_{CDOM}(440)$. However, these studies could not emphasize upon the spatial or annual variability of this relationship. In the present study, covering the entire annual cycle and nine evenly distributed sampling stations, it was found that the negative relationship between SSS and CDOM prevailed throughout the year ($R^2 = 0.80$; $p < 0.05$). Pandi et al. (2014) while working in the Bay of Bengal,

**Table 3** Relationship between CDOM absorption and salinity in a number of estuaries in the world.

| Study area | Equation | $R^2$ | Reference |
|---|---|---|---|
| nBoB | Salinity = $-32.4 \times a_{CDOM}(440) + 32.75$ | 0.80 | Present study |
| Northwestern Bay of Bengal, India | Salinity = $-90.9 \times a_{CDOM}(440) + 39.00$ | 0.77 | Pandi et al. (2014) |
| Pearl River, China | Salinity = $-125 \times a_{CDOM}(440) + 42.50$ | 0.98 | Hong et al. (2005) |
| Northwestern Mediterranean Sea, France | Salinity = $-31.3 \times a_{CDOM}(350) + 41.60$ | n/r | Para et al. (2010) |
| St. Lawrence Estuary, Canada | Salinity = $-1.87 \times a_{CDOM}(350) + 33.5$ | 0.99 | Xie et al. (2012) |
| Changjiang Estuary, China | Salinity = $-13.15 \times a_{CDOM}(355) + 33.08$ | 0.84 | Zhang et al. (2013) |
| Baltic Sea, Sweden | Salinity = $-2.63 \times a_{CDOM}(440) + 21.54$ | 0.87 | Harvey et al. (2015) |
| Swan River, Australia | Salinity = $-9.26 \times a_{CDOM}(440) + 45.37$ | n/r | Kostoglidis et al. (2005) |
| Baltic Sea | Salinity = $-5.88 \times a_{CDOM}(440) + 8.94$ | 0.88 | Kowalczuk et al. (2005) |
| Chesapeake Bay, USA | Salinity = $-111.1 \times a_{CDOM}(440) + 46.6$ | 0.67 | Rochelle-Newall and Fisher (2002) |
| Clyde Sea, Scotland | Salinity = $-12.19 \times a_{CDOM}(440) + 35.12$ | 0.99 | Binding and Bowers (2003) |
| Conwy, Wales | Salinity = $-10.0 \times a_{CDOM}(440) + 35.5$ | 0.98 | Bowers et al. (2004) |
| Canadian Arctic | Salinity = $-20.0 \times a_{CDOM}(440) + 32.2$ | 0.87 | Retamal et al. (2007) |

Key: $R^2$ = proportion of variance in CDOM absorption explained by linear regression on salinity, n/r = not recorded. All these equations are not present in the respective papers in such simplified form. Using the approach adopted by Bowers and Brett (2008) the above mentioned equations were formulated for most of the studies.

off Vishakhapatnam coast observed a similar negative relationship ($R^2 = 0.77$, $p < 0.05$). Many other studies carried out in riverine estuaries and plume systems of the world also observed that CDOM behaved conservatively and showed significant negative correlations with salinity (e.g., Bowers et al., 2004; Harvey et al., 2015; Hong et al., 2005; Para et al., 2010; Retamal et al., 2007; Siddorn et al., 2001; Xie et al., 2012; Zhang et al., 2013). Table 3 shows that the coefficient of determination of the relationship between SSS and CDOM observed in the Baltic Sea, estuaries of China, France, Australia, Canada and so forth were even better than that observed in the present study. The only exception was found to be the Chesapeake Bay, USA which recorded a lower $R^2$ of 0.67. Upon critically analysing the outcomes of Table 2, it can be seen that in the near shore stations (A and B transects), the relationship between SSS and CDOM values showed the high goodness of fit, whereas in the C transect (i.e. in the offshore stations) their relationship was not significant. Thus it can be deduced that in regions where the gradient and variability of salinity were higher, stronger correlations were observed and vice versa (Binding and Bowers, 2003). Binding and Bowers (2003) also observed that high river discharge having high CDOM constituents gives rise to a gradient in the SSS in such transition zones and hence leads to a strong relationship between SSS and $a_{CDOM}(440)$. The lower $a_{CDOM}(440)$ values and lack of variability of both SSS and $a_{CDOM}(440)$ observed at offshore stations might at the same time suggest a reduced river influence at the offshore stations. Similarly, upon analysing the seasonal variability irrespective of stations (Fig. 4), it was observed that the relationship between SSS and $a_{CDOM}(440)$ was much better during the monsoon season, i.e. when the salinity gradient was higher compared to the other two seasons (see y-axis of Fig. 4d–f).

Considering the spatial dynamics of $a_{CDOM}(440)$ it can be seen that the $a_{CDOM}(440)$ magnitudes slightly increased in the offshore stations (C1, C2, C3) during the post-monsoon season when a similar increase in chl-*a* concentrations were also observed (Fig. 2). This might be an indication of autochthonous CDOM production since chl-a magnitude indicates higher phytoplankton abundance which when degrades could act as a source of CDOM (Guo et al., 2011; Hong et al., 2012). Fig. 6 showed that relation between $a_{CDOM}(440)$ and TSM was much better in A1 ($R^2 = 0.83$, $p < 0.01$, SE = 0.13) than C3 ($R^2 = 0.68$, $p < 0.01$, SE = 0.18). River discharge and rainfall portray the intensity of riverine flow. The higher the riverine flow the higher happens to be the TSM. In this respect, it is observed that in the C transect, where the effect of riverine flow decreased substantially both the $a_{CDOM}(440)$ and TSM magnitudes diminished to a great extent (see the outliers of Fig. 4g–i). The observation of good correlation between $a_{CDOM}(440)$ and TSM was further testified by the observation that both river discharge and monthly mean rainfall correlated well with the $a_{CDOM}(440)$ variability observed in A1 (i.e. the most nearshore station) and the relationship degraded significantly in C3 (i.e. the most offshore station). Hence by virtue of the discussion made so far, we can again clearly accept the framed hypothesis of the present paper that this region exhibits significant spatial and temporal variability of $a_{CDOM}(440)$ and its primary driving factor is river-borne. Furthermore, the statistically significant negative correlation was observed between CDOM and SSS all through the annual cycle, however, it holds true only for the near shore stations (i.e. A and B transects). In the offshore stations this relationship was not found significant. Thus the third objective was also successfully fulfilled.

## 6. Conclusion

On the whole, it can be inferred that the nearshore to offshore transition zone in the nBoB portrayed significant spatial and temporal variability of coloured dissolved organic matter (CDOM) during one complete annual cycle. The CDOM in this region was mainly found to be of the allochthonous character and principally its source is river-borne. The magnitude of $a_{CDOM}(440)$ showed significant variation in the monsoon and non-monsoon season, with substantially higher magnitudes in monsoon season and lesser magnitude in

non-monsoon seasons. SSS exhibited a significantly strong negative relationship with $a_{CDOM}(440)$ throughout the year only in the nearshore stations. In the offshore stations this relationship was not found to be significant. During the post-monsoon season, when favourable conditions for photosynthetic activity prevailed in the water surface an increase in chl-*a* concentration was observed in the offshore stations along with a concurrent increase in $a_{CDOM}(440)$. This indicated an autochthonous character of CDOM during the post-monsoon season and that too only in the offshore stations. In future, fluorometric measurements of CDOM along with characterization of the CDOM sources and chemical composition of CDOM should be carried out in this region for better understanding.

## Acknowledgements

The study was funded by Indian National Centre for Ocean Information Services (INCOIS) (INCOIS: F&A: XII: A1:031), Ministry of Earth Sciences, India under Marine Fisheries Advisory Services (MFAS) programme. The authors are thankful to the Director of INCOIS for encouragement.

## References

Bidigare, R.R., Ondrusek, M.E., Brooks, J.M., 1993. Influence of the Orinoco River outflow on distributions of algal pigments in the Caribbean Sea. J. Geophys. Res. 98 (C2), 2259—2269, http://dx.doi.org/10.1029/92JC02762.

Binding, C.E., Bowers, D.G., 2003. Measuring the salinity of the Clyde Sea from remotely sensed ocean colour. Estuar. Coast. Shelf Sci. 57 (4), 605—611, http://dx.doi.org/10.1016/S0272-7714(02)00399-2.

Biswas, H., Dey, M., Ganguly, D., De, T.K., Ghosh, S., Jana, T.K., 2010. Comparative analysis of phytoplankton composition and abundance over a two-decade period at the land—ocean boundary of a tropical mangrove ecosystem. Estuar. Coast. 33 (2), 384—394, http://dx.doi.org/10.1007/s12237-009-9193-5.

Blough, N.V., Del Vecchio, R., 2002. Chromophoric DOM in the coastal environment. In: Hansell, D.A., Carlson, C.A. (Eds.), Biogeochemistry of Marine Dissolved Organic Matter. Acad. Press, Amsterdam, 509—546.

Blough, N.V., Green, S.A., 1995. Spectroscopic characterization and remote sensing of non-living organic matter. In: Zepp, R.G., Sonntag, C. (Eds.), The Role of Non-living Organic Matter in the Earth's Carbon Cycle. John Wiley and Sons, 23—45.

Blough, N.V., Zepp, R.G., 1990. Effects of solar ultraviolet radiation on biogeochemical dynamics in aquatic environments, Woods Hole Oceanographic Institution Technical Report. WHOI-90-09. 194 pp.

Bowers, D.G., Brett, H.L., 2008. The relationship between CDOM and salinity in estuaries: an analytical and graphical solution. J. Mar. Syst. 73 (1—2), 1—7, http://dx.doi.org/10.1016/j.jmarsys.2007.07.001.

Bowers, D.G., Evans, D., Thomas, D.N., Ellis, K., Williams, P.L.B., 2004. Interpreting the colour of an estuary. Estuar. Coast. Shelf Sci. 59 (1), 13—20, http://dx.doi.org/10.1016/j.ecss.2003.06.001.

Bricaud, A., Morel, A., Prieur, L., 1981. Absorption by dissolved organic matter of the sea (yellow substance) in the UV and visible domains. Limnol. Oceanogr. 26 (1), 43—53, http://dx.doi.org/10.4319/lo.1981.26.1.0043.

Carder, K.L., Steward, R.G., Harvey, G.R., Ortner, P.B., 1989. Marine humic and fulvic acids: their effects on remote sensing of ocean chlorophyll. Limnol. Oceanogr. 34 (1), 68—81, http://dx.doi.org/10.4319/lo.1989.34.1.0068.

Chen, H., Zheng, B., Song, Y., Qin, Y., 2011. Correlation between molecular absorption spectral slope ratios and fluorescence humification indices in characterizing CDOM. Aquat. Sci. 73 (1), 103—112, http://dx.doi.org/10.1007/s00027-010-0164-5.

Das, S., Chanda, A., Giri, S., Akhand, A., Hazra, S., 2015. Characterizing the influence of tide on the physico-chemical parameters and nutrient variability in the coastal surface water of the northern Bay of Bengal during the winter season. Acta Oceanol. Sin. 34 (12), 102—111, http://dx.doi.org/10.1007/s13131-015-0785-6.

Das, S., Hazra, S., Giri, S., Das, I., Chanda, A., Akhand, A., Maity, S., 2016b. Light absorption characteristics of chromophoric dissolved organic matter (CDOM) in the coastal waters of northern Bay of Bengal during winter season. Indian J. Geo-Mar. Sci. (in press).

Das, S., Hazra, S., Lotlikar, A.A., Das, I., Giri, S., Chanda, A., Akhand, A., Maity, S., Kumar, T.S., 2016a. Delineating the relationship between chromophoric dissolved organic matter (CDOM) variability and biogeochemical parameters in a shallow continental shelf. Egypt. J. Aquat. Res. 42 (3), 241—248, http://dx.doi.org/10.1016/j.ejar.2016.08.001.

De, T.K., De, M., Das, S., Chowdhury, C., Ray, R., Jana, T.K., 2011. Phytoplankton abundance in relation to cultural eutrophication at the land-ocean boundary of Sunderbans, NE Coast of Bay of Bengal, India. J. Environ. Stud. Sci. 1 (3), 169—180, http://dx.doi.org/10.1007/s13412-011-0022-3.

Del Castillo, C.E., Coble, P.G., 2000. Seasonal variability of the colored dissolved organic matter during the 1994—95 NE and SW monsoons in the Arabian Sea. Deep Sea Res. Pt. II: Topical Stud. Oceanogr. 47 (7—8), 1563—1579, http://dx.doi.org/10.1016/S0967-0645(99)00154-X.

Del Castillo, C.E., Gilbes, F., Coble, P.G., Müller-Karger, F.E., 2000. On the dispersal of riverine colored dissolved organic matter over the West Florida Shelf. Limnol. Oceanogr. 45 (6), 1425—1432, http://dx.doi.org/10.4319/lo.2000.45.6.1425.

Ferrari, G.M., 2000. The relationship between chromophoric dissolved organic matter and dissolved organic carbon in the European Atlantic coastal area and in the West Mediterranean Sea (Gulf of Lions). Mar. Chem. 70 (4), 339—357, http://dx.doi.org/10.1016/S0304-4203(00)00036-0.

Guo, W., Yang, L., Hong, H., Stedmon, C.A., Wang, F., Xu, J., Xie, Y., 2011. Assessing the dynamics of chromophoric dissolved organic matter in a subtropical estuary using parallel factor analysis. Mar. Chem. 124 (1—4), 125—133, http://dx.doi.org/10.1016/j.marchem.2011.01.003.

Harvey, E.T., Kratzer, S., Andersson, A., 2015. Relationships between colored dissolved organic matter and dissolved organic carbon in different coastal gradients of the Baltic Sea. Ambio 44 (Suppl. 3), 392—401, http://dx.doi.org/10.1007/s13280-015-0658-4.

Helms, J.R., Stubbins, A., Ritchie, J.D., Minor, E.C., Kieber, D.J., Mopper, K., 2008. Absorption spectral slopes and slope ratios as indicators of molecular weight, source, and photobleaching of chromophoric dissolved organic matter. Limnol. Oceanogr. 53 (3), 955—969, http://dx.doi.org/10.4319/lo.2008.53.3.0955.

Hong, H., Wu, J., Shang, S., Hu, C., 2005. Absorption and fluorescence of chromophoric dissolved organic matter in the Pearl River Estuary, South China. Mar. Chem. 97 (1—2), 78—89, http://dx.doi.org/10.1016/j.marchem.2005.01.008.

Hong, H., Yang, L., Guo, W., Wang, F., Yu, X., 2012. Characterization of dissolved organic matter under contrasting hydrologic regimes in a subtropical watershed using PARAFAC model. Biogeochemistry 109 (1), 163—174, http://dx.doi.org/10.1007/s10533-011-9617-8.

Jerlov, N.G., 1968. Optical Oceanography. American Elsevier Publ. Co., Inc., New York, 194 pp.

Karabashev, G.S., 1992. On the influence of dissolved organic-matter on remote-sensing of chlorophyll in the straits of Skagerrak and Kattegat. Oceanol. Acta 15 (3), 255—259.http://archimer.ifremer.fr/doc/00100/21159/.

Keith, D.J., Yoder, J.A., Freeman, S.A., 2002. Spatial and temporal distribution of coloured dissolved organic matter (CDOM) in Narragansett Bay, Rhode Island: implications for phytoplankton in coastal waters. Estuar. Coast. Shelf Sci. 55 (5), 705—717, http://dx.doi.org/10.1006/ecss.2001.0922.

Kirk, J.T.O., 1994. Light and Photosynthesis in Aquatic Ecosystems, 2nd ed. Cambridge Univ. Press, 510 pp.

Kostoglidis, A., Pattiaratchi, C.B., Hamilton, D.P., 2005. CDOM and its contribution to the underwater light climate of a shallow, macrotidal estuary in south-western Australia. Estuar. Coast. Shelf Sci. 63, 469—477, http://dx.doi.org/10.1016/j.ecss.2004.11.016.

Kowalczuk, P., Ston-Egiert, J., Cooper, W.J., Whitehead, R.F., Durako, M.J., 2005. Characterisation of chromophoric dissolved organic matter (CDOM) in the Baltic Sea by excitation emission matrix fluorescence. Mar. Chem. 96 (3—4), 273—292, http://dx.doi.org/10.1016/j.marchem.2005.03.002.

Lin, H., Guo, W., Hu, M., Lin, C., Ji, W., 2012. Spatial and temporal variability of colored dissolved organic matter absorption properties in the Taiwan Strait. Acta Oceanol. Sin. 31 (5), 98—106, http://dx.doi.org/10.1007/s13131-012-0240-x.

Loiselle, S.A., Bracchini, L., Dattilo, A.M., Ricci, M., Tognazzi, A., Cózar, A., Rossi, C., 2009. The optical characterization of chromophoric dissolved organic matter using wavelength distribution of absorption spectral slopes. Limnol. Oceanogr. 54 (2), 590—597, http://dx.doi.org/10.4319/lo.2009.54.2.0590.

Luyten, P.J., Deleersnijder, E., Ozer, J., Ruddick, K.G., 1996. Presentation of a family of turbulence closure models for stratified shallow water flows and preliminary application to the Rhine outflow region. Cont. Shelf Res. 16 (1), 101—130, http://dx.doi.org/10.1016/0278-4343(95)93591-V.

Maneesha, K., Sarma, V.V.S.S., Reddy, N.P.C., Sadhuram, Y., Murty, T.R., Sarma, V.V., Kumar, M.D., 2011. Meso-scale atmospheric events promote phytoplankton blooms in the coastal Bay of Bengal. J. Earth Syst. Sci. 120 (4), 773—782, http://dx.doi.org/10.1007/s12040-011-0089-y.

Morel, A., 1988. Optical modeling of the upper ocean in relation to its biogenous matter content (Case I waters). J. Geophys. Res. 93 (C9), 10749—10768, http://dx.doi.org/10.1029/JC093iC09p10749.

Mukhopadhyay, S.K., Biswas, H.D.T.K., De, T.K., Jana, T.K., 2006. Fluxes of nutrients from the tropical River Hooghly at the land—ocean boundary of Sundarbans, NE Coast of Bay of Bengal, India. J. Mar. Syst. 62 (1—2), 9—21, http://dx.doi.org/10.1016/j.jmarsys.2006.03.004.

Pandi, S.R., Kiran, R., Sarma, N.S., Srikanth, A.S., Sarma, V.V.S.S., Krishna, M.S., Bandyopadhyay, D., Prasad, V.R., Acharyya, T., Reddy, K.G., 2014. Contrasting phytoplankton community structure and associated light absorption characteristics of the western Bay of Bengal. Ocean Dyn. 64 (1), 89—101, http://dx.doi.org/10.1007/s10236-013-0678-1.

Para, J., Coble, P.G., Charrière, B., Tedetti, M., Fontana, C., Sempéré, R., 2010. Fluorescence and absorption properties of chromophoric dissolved organic matter (CDOM) in coastal surface waters of the northwestern Mediterranean Sea, influence of the Rhône River. Biogeosciences 7 (12), 4083—4103, http://dx.doi.org/10.5194/bg-7-4083-2010.

Parson, T.R., Maita, Y., Lalli, C.M., 1984. A Manual of Chemical and Biological Methods for Seawater Analysis. Pergamon Press, New York, p. 173.

Pegau, W.S., Zaneveld, J.R.V., 1993. Temperature-dependent absorption of water in the red and near-infrared portions of the spectrum. Limnol. Oceanogr. 38 (1), 188—192, http://dx.doi.org/10.4319/lo.1993.38.1.0188.

Retamal, L., Vincent, W.F., Martineau, C., Osburn, C.L., 2007. Comparison of the optical properties of dissolved organic matter in two river-influenced coastal regions of the Canadian Arctic. Estuar. Coast. Shelf Sci. 72 (1), 261—272, http://dx.doi.org/10.1016/j.ecss.2006.10.022.

Rochelle-Newall, E.J., Fisher, T.R., 2002. Chromophoric dissolved organic matter and dissolved organic carbon in Chesapeake Bay. Mar. Chem. 77 (1), 23—41, http://dx.doi.org/10.1016/S0304-4203(01)00073-1.

Rudra, K., 2014. Changing river courses in the western part of the Ganga—Brahmaputra delta. Geomorphology 227, 87—100, http://dx.doi.org/10.1016/j.geomorph.2014.05.013.

Sasaki, H., Miyamura, T., Saitoh, S.I., Ishizaka, J., 2005. Seasonal variation of absorption by particles and colored dissolved organic matter (CDOM) in Funka Bay, southwestern Hokkaido, Japan. Estuar. Coast. Shelf Sci. 64 (2), 447—458, http://dx.doi.org/10.1016/j.ecss.2005.03.008.

Siddorn, J.R., Bowers, D.G., Hoguane, A.M., 2001. Detecting the Zambezi River plume using observed optical properties. Mar. Pollut. Bull. 42 (10), 942—950, http://dx.doi.org/10.1016/S0025-326X(01)00053-4.

Stedmon, C.A., Markager, S., Kaas, H., 2000. Optical properties and signatures of chromophoric dissolved organic matter (CDOM) in Danish coastal waters. Estuar. Coast. Shelf Sci. 51 (2), 267—278, http://dx.doi.org/10.1006/ecss.2000.0645.

Strickland, J.D., Parsons, T.R., 1972. A Practical Handbook of Seawater Analysis, 167 pp.

Suzuki, R., Ishimaru, T., 1990. An improved method for the determination of phytoplankton chlorophyll using N,N-dimethylformamide. J. Oceanogr. 46 (4), 190—194, http://dx.doi.org/10.1007/BF02125580.

Tassan, S., 1988. The effect of dissolved "yellow substance" on the quantitative retrieval of chlorophyll and total suspended sediment concentrations from remote measurements of water colour. Remote Sens. 9 (4), 787—797, http://dx.doi.org/10.1080/01431168808954893.

Unger, D., Ittekkot, V., Schäfer, P., Tiemann, J., Reschke, S., 2003. Seasonality and interannual variability of particle fluxes to the deep Bay of Bengal: influence of riverine input and oceanographic processes. Deep-Sea Res. II: Topical Stud. Oceanogr. 50 (5), 897—923, http://dx.doi.org/10.1016/S0967-0645(02)00612-4.

Varkey, M.J., Murty, V.S.N., Suryanarayana, A., 1996. Physical oceanography of the Bay of Bengal and Andaman Sea. In: Ansell, A.D., Gibson, R.N., Barnes, M. (Eds.), Oceanography and Marine Biology. UCL, London, 1—70.

Vodacek, A., Blough, N.V., DeGrandpre, M.D., Peltzer, E.T., Nelson, R.K., 1997. Seasonal variation of CDOM and DOC in the Middle Atlantic Bight: terrestrial inputs and photooxidation. Limnol. Oceanogr. 42 (4), 674—686, http://dx.doi.org/10.4319/lo.1997.42.4.0674.

Xie, H., Aubry, C., Bélanger, S., Song, G., 2012. The dynamics of absorption coefficients of CDOM and particles in the St. Lawrence estuarine system: biogeochemical and physical implications. Mar. Chem. 128—129, 44—56, http://dx.doi.org/10.1016/j.marchem.2011.10.001.

Zhang, X.Y., Chen, X., Deng, H., Du, Y., Jin, H.Y., 2013. Absorption features of chromophoric dissolved organic matter (CDOM) and tracing implication for dissolved organic carbon (DOC) in Changjiang Estuary, China. Biogeosci. Discuss. 10, 12217—12250, http://dx.doi.org/10.5194/bgd-10-12217-2013.